Journal of Materials Chemistry C

Accepted Manuscript

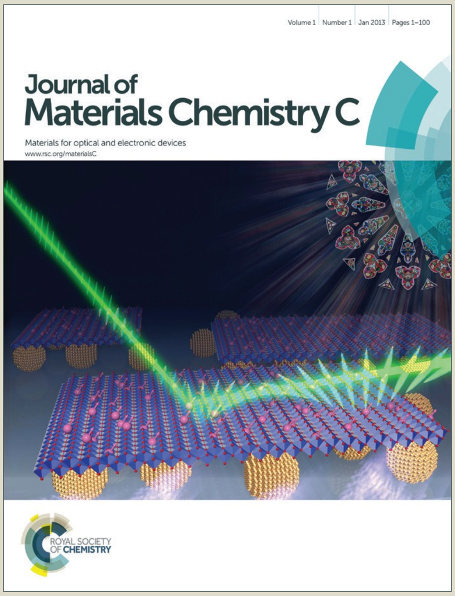

ROYAL SOCIETY OF CHEMISTRY

www.rsc.org/materialsC

Journal Name

ARTICLE

Blue-emitting phosphor Ba_4OCl_6: Eu^{2+} with good thermal stability and tiny chromaticity shift for white LEDs

cReceived 00th January 20xx,
Accepted 00th January 20xx

DOI: 10.1039/x0xx00000x

www.rsc.org/

Yan Chen, Fengjuan Pan, Meng Wang, Xuejie Zhang, Jing Wang*, Mingmei Wu* and Chengxin Wang

An intense blue-emitting phosphor, Ba_4OCl_6: Eu^{2+}, was developed by solid state reaction at low synthesis temperature. The photoluminescence excitation and emission spectra, concentration effect, thermal-dependent luminescence quenching properties, chromaticity shift, activity energy and luminous efficiency of the radiation are investigated. These results show that Eu^{2+} exhibits a broadband excitation extending from 250 to 400 nm and emits an intense blue light at 450 nm with tiny colour chromaticity shift at temperature range of 350-490 K. The external quantum efficiency of $Ba_{3.97}OCl_6$: $Eu^{2+}_{0.03}$ is about 26.6 %. It demonstrates that Eu^{2+} doped Ba_4OCl_6 can be excited by n-UV LEDs chip and is an effective blue-emitting phosphor potentially useful in white LEDs.

1. Introduction

Phosphor converted white light emitting diodes (pc-LEDs) have attracted more and more attention and are considered to be the next generation lighting source because of its high efficiency, energy-saving, environment-friendly, long lifetime and so on [1]. Nowadays, a blue LEDs chip coated with a yellow-emitting phosphor (YAG: Ce^{3+}) is still the main method for fabricating commercial white LEDs. However, this design has some disadvantages such as low colour-rendering index (CRI) of Ra < 80 and high correlated colour temperature (CCT) of < 4500 K, because of the lack of red light component in the emission of yellow phosphor [2]. Therefore, tricolours phosphors pumped by ultraviolet LED chip is strongly expected to be an effective approach to get excellent CRI and high CCT white light [3].

Nowadays, $BaMgAl_{10}O_{17}$: Eu^{2+} (BAM) is used as the commercial blue-emitting phosphor. Unfortunately, it is commonly synthesized by traditional solid state method and the calcination temperature is high up to 1600 °C [4]. Even added AlF_3 as flux, the synthesis temperature is still about 1400 °C [5]. Furthermore, BAM suffers from obvious chromaticity shift with the increasing of test temperature, which makes the colour of the white LEDs device inconsistent. Hence, it is vital to reduce the reaction temperature and improve the chromaticity shift of blue-emitting phosphor for white LEDs.

In this article, a series of blue-emitting phosphors, $Ba_{4-x}OCl_6$: Eu^{2+}_x, were prepared by conventional solid-state reaction at low sintering temperature. Crystalline structure and composition, photoluminescence properties, activation energy, chromaticity shift, luminous efficiency of the radiation and so on, were investigated in detail. It is demonstrated that this phosphor can be efficiently excited by (n)-UV LEDs chip and emits intense blue light with good thermal stability and tiny chromaticity shift.

2. Experiment

2.1 Syntheses: All the samples $Ba_{4-x}OCl_6$:Eu^{2+}_x (x=0, 0.01, 0.03, 0.05, 0.07, 0.09) were prepared by a conventional solid-state reaction technique. Firstly, the starting materials, $BaCl_2 \cdot 2H_2O$ (A.R.), $BaCO_3$ (A.R.) and Eu_2O_3 (99.99%) were weighed in stoichiometric amounts. Subsequently, the powder mixture was thoroughly mixed in an agate mortar by grinding and was transferred into crucibles. Finally, they were sintered at 700 °C for 8 h under a N_2/H_2 atmosphere and cooled to room temperature naturally. The sintered samples were ground into powders for measurement.

2.2 Measurements: The phase purity of the prepared phosphors was investigated by Bruker D8 advance X-ray diffractometer (XRD) with Cu Ka (λ=1.5405 Å) radiation at 40 kV and 40 mA. High quality XRD data for Rietveld refinement was collected over a 2θ range from 5° to 110° at an interval of 0.02°. Structural refinement of XRD data was performed using the TOPAS-Academic program [6].

The photoluminescence (PL), photoluminescence excitation (PLE) spectra, temperature-dependent PL spectra and the decay curves at room temperature were measured by FSP920 Time Resolved and

---

State Key Laboratory of Optoelectronic Materials and Technologies, School of Physics and Engineering, School of Chemistry and Chemical Engineering, Sun Yat-sen University Guangzhou, Guangdong 510275, P.R. China.
Fax: (+86) 20-84112112
**E-mail: ceswj@mail.sysu.edu.cn; ceswmm@mail.sysu.edu.cn.*
Electronic Supplementary Information (ESI) available: [details of any supplementary information available should be included here]. See DOI: 10.1039/x0xx00000x

Steady State Fluorescence Spectrometers (Edinburgh Instruments) equipped with a 450 W Xe lamp, a 150W nF 900 flash lamp, TM300 excitation monochromator and double TM300 emission monochromator, Red sensitive PMT and R5509-72 NIR-PMT in a liquid nitrogen cooled housing (Hamamatsu Photonics K.K). The spectral resolution is about 0.05 nm in UV-VIS.

For the PL spectra in the temperature range of 77-490 K and decay measurement in temperature 77 K to 300 K, the powder sample was mounted in an Optstat DNV actively cooled optical cryostat with an ITC601 temperature controller.

The quantum efficiency of the as-prepared phosphor and BAM were measured by QY-2000 equipped with a 450 W Xe lamp. The standard reference is Al_2O_3.

The morphology and elemental composition of the as-prepared products were measured by SEM (Scanning electron microscope) (FEI Quanta 400).

Table 1. Final refined structural parameters for $Ba_{3.97}OCl_6$: $Eu^{2+}_{0.03}$

atom	site	x	y	z	occupancy	Bio(Å2)
Ba1	6c	0.19497(6)	0.3899(2)	0.007(3)	1	1.36(2)
Ba2	2b	1/3	2/3	0.441(4)	1	1.12(5)
Cl1	6c	0.1417(3)	0.2834(6)	0.306(3)	1	2.5(1)
Cl2	6c	0.4698(3)	0.5301(3)	0.724(4)	1	2.1(1)
O1	2b	1/3	2/3	0.092(3)	1	2.7(7)

3. Results and discussion

3.1 Phase Characterization

The Rietveld refinement was performed on the XRD pattern of the $Ba_{3.97}OCl_6$: $Eu^{2+}_{0.03}$ upon the structural model of Ba_4OCl_6 [7] via TOPAS ACADEMIC software, whose standard pattern is JCPDS 72-0630. The fitted results of the observed and calculated X-ray diffraction data and the difference are presented in Fig. 1 (a) with good reliability factors converged to R_{wp}=3.41% and R_p=2.04%, which indicates the single phase of $Ba_{3.97}OCl_6$: $Eu^{2+}_{0.03}$ is obtained and the doping of Eu^{2+} did not cause any impurities. The final refined results confirm that $Ba_{3.97}OCl_6$: $Eu^{2+}_{0.03}$ crystalizes in a space group of $P6_3mc$, with fitted lattice parameters of a=9.9757(1) Å, c=7.5429(1) Å, Z = 2. Figure 1b shows the perspective view of the unit cell along the c axis. The host contains two types of Ba sites with high asymmetry, namely Ba1 and Ba2, respectively. The Ba1 has a coordination number of eight with seven Cl atoms and one O atom, while the coordination of Ba2 site is composed of six Cl atoms and one O atom. It is reported that the effective ionic radius of Eu^{2+} ion and Ba^{2+} ion are 1.25 Å and 1.47 Å at CN=8 and 1.20 Å and 1.38 Å at CN = 7. Furthermore, they have the same valence state. It is obvious that the ionic radius of Eu^{2+} ion is close to Ba^{2+} ion. These results suggest that Eu^{2+} prefer to occupy Ba^{2+} site randomly in the present host [8]. The final atomic coordinates are illustrated in table 1.

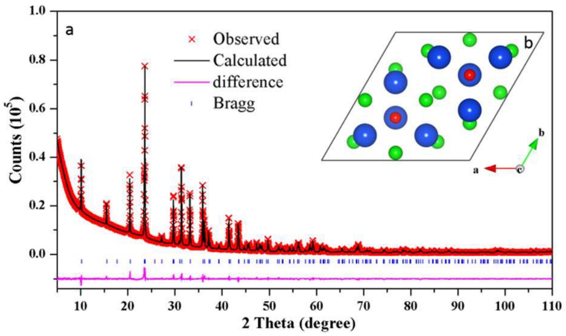

Fig. 1 Observed (crosses), calculated (solid line), and difference (bottom) results of XRD refinement of $Ba_{3.97}OCl_6$: $Eu^{2+}_{0.03}$

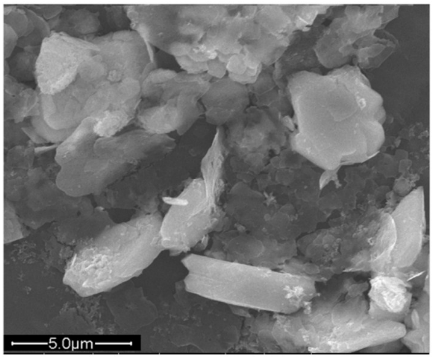

Fig. 2 SEM images of the Ba_4OCl_6

3.2 Morphology Characterization and composition

The surface morphology and composition of Ba_4OCl_6 was well examined by SEM and Energy–dispersive X-ray (EDX) spectrum. Many in-homogenous particles with different length are found in Fig. 2. EDX spectrum was employed to roughly characterize chemical composition of this compound. The atomic ratio of barium (Ba), oxygen (O) and chlorine (Cl) is about 4: 1: 7, which is closes to the stoichiometric composition of molecular formula of Ba_4OCl_6.

3.3 Luminescence properties

Fig. 3 (a) depicts that the PL spectra of $Ba_{4-x}OCl_6$: Eu^{2+}_x contains a broad band at 400-650 nm which belongs to allowed 5d→4f transition of Eu^{2+} ion in this host. However, the band is asymmetric, which means there is more than one site of Eu^{2+}. Combined the matrix structure, we deduce that there is two Eu^{2+} sites and will discuss in detail by the low temperature spectra. The band peaked at 450 nm is assigned to the site of Eu1 and peaked at 540 nm is Eu2. Unlike the PL spectra, there is a broad excitation band at 250-425 nm in the PLE spectrum, whether monitoring the emission of Eu1 or Eu2. It means this phosphor can be effectively excited by UV LED chip effectively. In all, the appearance of the 4f−5d absorption transition of Eu1, monitoring emission of Eu2 (540 nm), and 5d−4f radiative transition of Eu2 excited to Eu1 suggest that the energy transfer from Eu1 to Eu2 is possible.

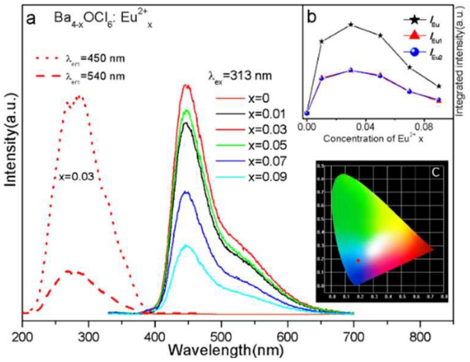

Fig. 3 PLE and PL spectra of $Ba_{4-x}OCl_6$: Eu^{2+}_x (a). Inset is the concentration dependence of integrated emission intensities of Eu^{2+} ion (b) and chromaticity coordinates of $Ba_{3.97}OCl_6$:$Eu^{2+}_{0.03}$ under 313 nm excitation(c)

It is interesting that the shape and the peak of the emission band remain the same with the increasing of the Eu^{2+} concentration. The integrated emission intension of Eu, Eu1 and Eu2 all firstly increases, then reaches a maximum at x = 0.03 and finally decreases, as shown is Fig. 3 (c). It suggests that Eu^{2+} occupy both Ba1 site and Ba2 site by a certain proportion and the energy transfer efficiency keeps the same with the increasing of concentration of Eu^{2+}. The chromaticity coordinates of $Ba_{4-x}OCl_6$: Eu^{2+}_x are almost the same with the changing of concentration of Eu^{2+}, which is depicted in Fig. 3(c).

In order to understand the concentration quenching mechanism, it is essential to calculate the critical distance (R_c) of the Eu^{2+} activator ion. It can be estimated by the following equation [9]

$$R_c \approx 2\left[\frac{3V}{4\pi X_c\ N}\right]^{1/3} \qquad (1)$$

where X_c is the critical concentration, N the number of cation in the unit cell and V the volume of the unit cell. Using the known structural parameter values of V = 751.38 Å^3, N = 4, and X_c = 0.03/4, R_c was calculated to be about 36.31 Å. The resonant energy transfer mechanism consists of two types: exchange or multipolar interaction [10]. For the exchange interaction, R_c is generally shorter than 3–4 Å. In $Ba_{3.97}OCl_6$: $Eu^{2+}_{0.03}$, the distance between Eu^{2+} ions is about 36.31 Å in this phosphor, which is much larger than R_c for the exchange interaction. Therefore, the concentration quenching mechanism in Ba_4OCl_6: Eu^{2+} is considered to be the multipolar interaction.

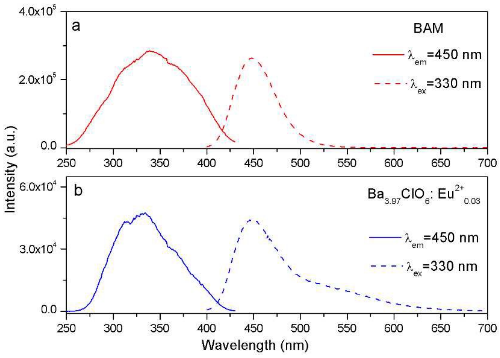

Fig. 4 PLE and PL spectra of BAM and $Ba_{3.97}OCl_6$: $Eu^{2+}_{0.03}$ (λ_{em}=450 nm, λ_{ex}=330 nm).

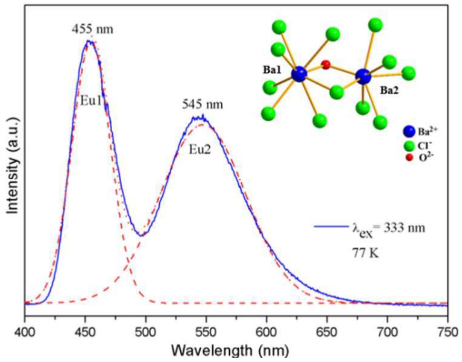

Fig. 5 PLE spectra of $Ba_{3.97}OCl_6$:$Eu^{2+}_{0.03}$ at 77 K (the red dash lines are fitted curves). Insert is representing two crystallographic Ba sites, where blue, green, and red spheres are Ba, Cl, and O atoms, respectively.

Fig. 4 shows the comparison of the PLE and PL spectra of BAM and $Ba_{3.97}OCl_6$: $Eu^{2+}_{0.03}$. They both have a broad band at 250-425 nm, which means they all can be excited by UV-LED chip effectively. When excited by 330 nm, there are an emission band of $Ba_{3.97}OCl_6$: $Eu^{2+}_{0.03}$ peaked at 450 nm as same as BAM. However, the integrated emission intensity of $Ba_{3.97}OCl_6$: $Eu^{2+}_{0.03}$ is about 25.6 % of BAM. The intensity of $Ba_{4-x}OCl_6$: Eu^{2+}_x could be improved by adding the flux, adjusting the calcination temperature or time.

The quantum efficiency of is one of the important standards for evaluation of phosphor. $Ba_{3.97}OCl_6$:$Eu^{2+}_{0.03}$ and BAM were recorded using an integrating sphere attached to a Hitachi F7000 spectrofluorometer. The external quantum efficiency of $Ba_{3.97}OCl_6$: $Eu^{2+}_{0.03}$ and BAM are about 20.74 % and 77.98 % under 330 nm exciting, respectively. In other words, the external quantum efficiency of $Ba_{3.97}OCl_6$: $Eu^{2+}_{0.03}$ is about 26.6 % of commercial phosphor BAM, which is in line with their integrated emission intensity ratio of $Ba_{3.97}OCl_6$: $Eu^{2+}_{0.03}$ to BAM.

As shown in Fig. 3, the emission spectra are broad and asymmetric, which illustrates the Eu^{2+} are derived from different sites in matrix of Ba_4OCl_6. The Ba atoms form two polyhedral units and connect with Cl and O atom with eight- and seven-coordination, marked as Ba1 ($BaOCl_7$) and Ba2 ($BaOCl_6$), respectively. Therefore, Eu^{2+} may occupies two types of Ba sites in this phosphor and marked as Eu1 and Eu2. The crystal field of Ba1 is weaker than Ba2, because of the high coordination number of Ba1, as discussed above. As a consequence, the emission wavelength of Eu2 is longer than Eu1, according to the relatively lower energy of the lowest 5d of Eu2. In order to deeply study the site occupy of Eu^{2+} in this matrix, PLE spectrum of $Ba_{3.97}OCl_6$: $Eu^{2+}_{0.03}$ at 77 K is present in Fig. 5. There are obviously two emission bands peaked at 455 nm and 545 nm, which are attributed to Eu^{2+} in site of Ba1 and Ba2, respectively. The results is well match with the reference [11].

Generally, the PL decay times of active ion are similar, when it occupy the same site. In order to well study the two sites emission of Eu^{2+}, Fig. 6 show the PL decay curves of $Ba_{3.97}OCl_6$: $Eu^{2+}_{0.03}$ at 77K. Fig. 6 (a, b) and (c, d) present the emission decay at 450 nm and 540 nm of Eu^{2+} in site 1 and site 2 upon excitation at 313 nm, 330 nm, respectively. The decay behaviour can be expressed as follows [12]:

$$I = A \exp(-t/\tau) + I_0 \qquad (2)$$

where I and I_0 are emission intensity, A is constant, t is time and τ is decay time for exponential component. It is calculated that whatever the excitation wavelength are monitored, the lifetime of Eu^{2+} at 450 nm and 540 nm are about 1.380 μs and 1.360 μs, and 1.345 μs and 1.341 μs, which also means there is two Eu^{2+} sites. It is clear that the lifetime of Eu^{2+} about 1.3 μs in site 2 is slightly shorter than 1.4 μs site 1, which is attributed to the slightly different coordination environment of Eu^{2+} at Eu1 and Eu2 sites. The surrounding of Eu1 is relatively looser than Eu2, which may leads to stronger electron-phonon interactions between Eu1 ion and O/Cl anions and consequently results in fast depopulation of excited Eu1 ion, i.e., the decreasing lifetime of Eu1 ion.

3.4 Thermal stability

Thermal quenching property of phosphor is of great significance for its application in LEDs under high operation junction temperature. Fig. 7 (a) presents the PL spectra of $Ba_{3.97}OCl_6$: $Eu^{2+}_{0.03}$ at the temperature range of 77- 490 K. In order to well study the thermal quenching property of Eu1 and Eu2, Fig. 7 (b) shows the temperature-dependent integrated emission intensities of Eu1and Eu2. It is clearly observed that the integrated emission intensity of Eu1 increases, then reaches a maximum at 250 K and finally decreases, and Eu2 gradually decreases with the temperature rising. Such different quenching behaviour between Eu1 and Eu2 maybe is due to the balance between the energy transfer from Eu2 to Eu1 and thermal quenching of themselves. As shown in Fig. 5, the lowest 5d level of Eu1 and Eu2 is about 21978 cm^{-1} and 18349 cm^{-1}, respectively. The difference is 3624 cm^{-1}. As usual, the stretching vibration frequency of Cl-O chlorate is about 910 cm^{-1} [13]. It is expected that the energy difference between the lowest 5d level of Eu1 and Eu2 is bridged by phonons in the host, which demonstrates that the energy transfer from Eu2 to Eu1 is efficient at the temperature range of 77-250 k, and the thermal quenching efficiency is prominent at 250-490 K, which leads to that the integrated emission intensity of Eu1 increases at first and then decreases. In addition, both the energy transfer from Eu2 to Eu1 and thermal quenching of Eu2 itself results in the decrease of integrated emission intensity of Eu2 with temperature rising. The inset of Fig. 7 (b) gives the ratios of integrated emission intensities of Eu1 and Eu2 at 423k to at 298k, i.e., I_{423K}/ I_{298K}. Compared with the intensity at room temperature, the integrated emission intensity at 423 K of Eu1 and Eu2 are about 73.1 % and 77.7 %, respectively. It means that the thermal quenching of Eu1 is more quickly than Eu2, which may be due to looser coordination environment of Eu1 than Eu2 and consequently stronger electron-phono interactions of Eu1 than Eu2.

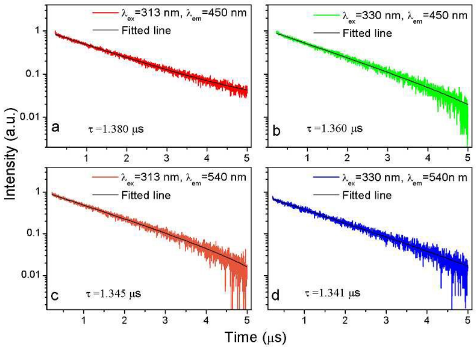

Fig. 6 PL decay curves of $Ba_{3.97}OCl_6$:$Eu^{2+}_{0.03}$ at 77 K (colour lines are the experiment data; black lines are the fitted curves)

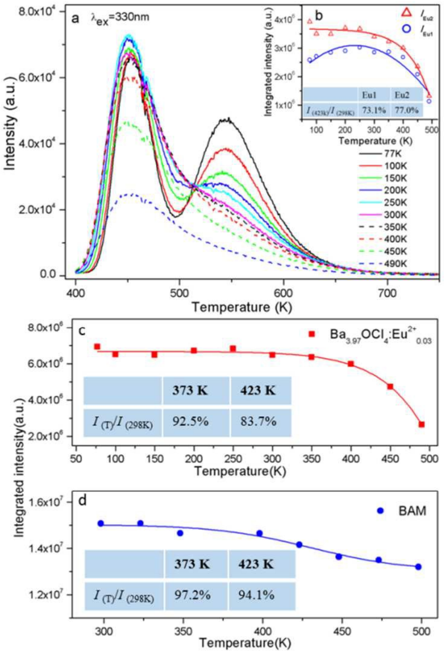

Fig. 7 The PL spectra of $Ba_{3.97}OCl_6$: $Eu^{2+}_{0.03}$ at the temperature range of 77-490 K (a); Temperature-dependent integrated emission intensities of Eu1 and Eu2 (b), $Ba_{3.97}OCl_6$: $Eu^{2+}_{0.03}$ (c), and BAM (d)

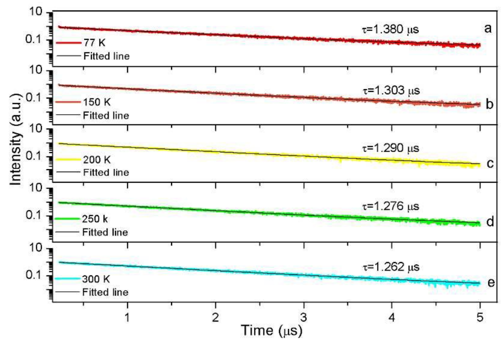

Fig. 8 PL decay curves of $Ba_{3.97}OCl_6$:$Eu^{2+}_{0.03}$ in different temperature (λ_{ex}=313 nm, λ_{em}=450 nm); colour lines are the experiment data; black lines are the fitted curves)

In order to further study the thermal quenching property, Fig. 7 (c and d) shows the temperature-dependent integrated emission intensity of $Ba_{3.97}OCl_6$: $Eu^{2+}_{0.03}$ and BAM. The integrated emission intensity of BAM decreases marginally with the temperature rising from 300 K to 500 K and remains 97.2 % and 94.1% at 373 K and 423 K. It is clearly that integrated emission intensity of $Ba_{3.97}OCl_6$: $Eu^{2+}_{0.03}$ decreases gently with the temperature rising from 77 K to 490 K and then reduces sharply, because of the larger non-radiative transition probability at higher temperature. Compared with the intensity at room temperature, the integrated emission intensity at 373 K and 423 K still remains 92.57% and 83.7%, respectively. The results above means that $Ba_{3.97}OCl_6$: $Eu^{2+}_{0.03}$ has a good temperature quenching characteristics and is a promising candidate for pc-LEDs.

Fig. 8 presents the PL decay curves of $Ba_{3.97}OCl_6$:$Eu^{2+}_{0.03}$ in deferent temperature. The lifetimes of Eu^{2+} are 1.380μs, 1.303μs, 1.290μs, 1.276μs and 1.262μs for the samples at 77 K, 150 K, 200 K, 250 K and 300 K. The decrease in the lifetime of Eu^{2+} with increasing temperature indicates that Eu^{2+} ion undergoes stronger and stronger electron-phonon interactions.

3.5 Activation energy and Chromaticity shift

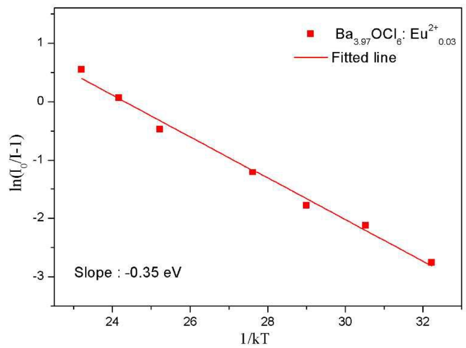

Fig. 9 Plot of ln(I_0/I − 1) vs 1/kT activation energy for thermal quenching of the characteristic emission of $Ba_{3.97}OCl_6$:$Eu^{2+}_{0.03}$.

Table 2. The activation energy (*E*a) of some published phosphor

phosphor	*E*a	Ref.
$K_2Al_2B_2O_7$: Eu^{2+}	0.30 eV	15
α-$Ca_{1.60}Sr_{0.35}SiO_4$: $0.05Ce^{3+}$	0.14 eV	16
$Sr_5Cl_{0.75}F_{0.25}(PO_4)_3$: Eu^{2+}	0.22 eV	17
$KBaPO_4$: Eu^{2+}	0.12 eV	18
$NaBaPO_4$: Eu^{2+}	0.05 eV	18
$(Ca_{0.94}Ce_{0.03}Li_{0.03})_3Si_2O_4N_2$:$Ce^{3+}$,$Li^+$	0.05 eV	19
$Ca_5(PO_4)_3Cl$:Eu^{2+}	0.02 eV	19

To further understanding the relation between emission intensity and temperature, the activation energy was estimated by the Arrhenius equation [14]:

$$I(T) \approx \frac{I_0}{1+c\exp\left(\frac{-\Delta E}{kT}\right)} \qquad (3)$$

in which I_0 and *I(T)* are the initial luminescence intensity of the sample at room temperature and the testing temperature, respectively, Δ*E* is the activation energy for the thermal quenching, c is a constant, and k is the Boltzman's constant (8.62×10^{-5} eV K^{-1}). Activation energy is energy level difference between the lowest energy level of relaxed excited level and the host lattice conduction band. Therefore, in the same or similar crystal structure, the larger the activation energy Δ*E* is, the better the thermal stability will be. As shown in Fig. 9, Δ*E* of $Ba_{3.97}OCl_6$:$Eu^{2+}_{0.03}$ can be calculated via plotting ln(I_0/I − 1) against 1/kT and is 0.35 eV. At the same time, Table 2 gives the activation energy (*E*a) of some phosphors previous published. One of the influence factors to activation energy maybe is the phonon vibrations frequency of the host. The higher phonon frequency, the bigger activation energy is. The relatively high activation energy indicates good thermal stability for $Ba_{3.97}OCl_6$:$Eu^{2+}_{0.03}$, which means it is a candidate of blue emitting phosphor for white LEDs [15].

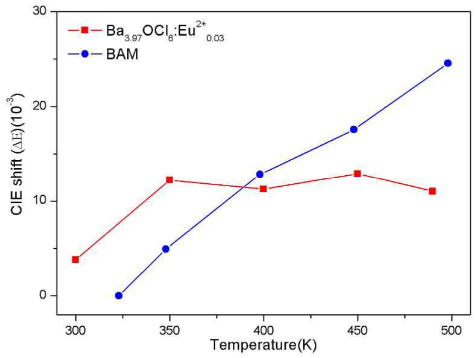

Fig. 10 Chromaticity shift of the commercial blue-emitting phosphor BAM and $Ba_{3.97}OCl_6$:$Eu^{2+}_{0.03}$ (λ_{ex} = 370 nm)

Table 3. CIE chromaticity coordinates of the commercial blue-emitting phosphor BAM and $Ba_{3.97}OCl_6$:$Eu^{2+}_{0.03}$ (BOC) (λ_{ex}=370 nm)

T (K)	(x, y) (BAM)	T (K)	(x, y) (BOC)
298	(0.143, 0.068)	300	(0.201, 0.210)
348	(0.143, 0.070)	350	(0.199, 0.209)
398	(0.144, 0.073)	400	(0.196, 0.208)
448	(0.144, 0.075)	450	(0.194, 0.208)
498	(0.144, 0.077)	490	(0.196, 0.214)

The chromaticity coordination at different temperature is an important parameter for studying the property of light source. CIE chromaticity coordinates of commercial blue-emitting phosphor BAM and $Ba_{3.97}OCl_6$:$Eu^{2+}_{0.03}$ at different temperature are depicted in Table 3. Chromaticity shift (ΔE) was calculated by the following equation: [20]

$$\Delta E = \sqrt{(u'_t - u'_0)^2 + (v'_t - v'_0)^2 + (w'_t - w'_0)^2} \qquad (4)$$

where u′= 4x/(3 − 2x + 12y), v′= 9y/(3 − 2x + 12y), and w′= 1 − u′ − v′. The u′ and v′ are the chromaticity coordinates in u′ v′ uniform colour space, x and y are the chromaticity coordinates in CIE 1931 colour space, and 0 and t are the chromaticity shift at 298 K and a given temperature, respectively. As shown in Fig. 10, the chromaticity shift of commercial blue-emitting phosphor BAM gradually increases with the temperature rising and is 1.52×10^{-2} at 423 K. However, the chromaticity shift of phosphor $Ba_{3.97}OCl_6$: $Eu^{2+}_{0.03}$ firstly increases until 350 K, then remains the same with the temperature rising again and is 1.21×10^{-2} at 423 K. It means the chromaticity shift of phosphor $Ba_{3.97}OCl_6$:$Eu^{2+}_{0.03}$ is smaller than BAM. The results shows that phosphor $Ba_{3.97}OCl_6$: $Eu^{2+}_{0.03}$ can keep good colour consistency for whit LEDs device and is better than the commercial blue-emitting phosphor BAM

3.6 Luminous efficiency

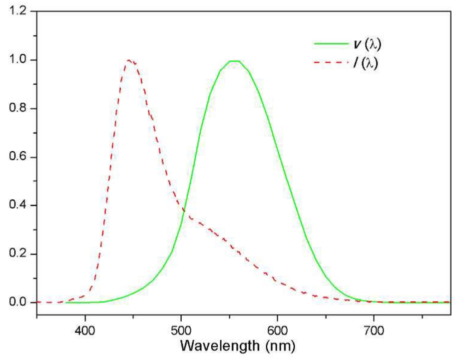

Fig. 11 The normalized spectral eye sensitivity cures for photopic vision *V* (λ) and spectrum of phosphor $Ba_{3.97}OCl_6$: $Eu^{2+}_{0.03}$ *I* (λ)

The luminous efficiency of the radiation (LER) is an important parameter which shows how bright the radiation is perceived by the average human eye. Fig. 11 shows the normalized spectral eye sensitivity cures for photopic vision and spectrum of phosphor $Ba_{3.97}OCl_6$:$Eu^{2+}_{0.03}$. It can be calculated from the emission spectrum as: [21]

$$\mathrm{LER}(lm/w) = 683\ lm/w \cdot \frac{\int_{380\ nm}^{780\ nm} I(\lambda)V(\lambda)d\lambda}{\int_{380\ nm}^{780\ nm} I(\lambda)d\lambda} \qquad (4)$$

where *V (λ)* and *I (λ)* are eye sensitivity cure and phosphor emission spectrum respectively. The *LER* of the $Ba_{3.97}OCl_6$:$Eu^{2+}_{0.03}$ is 23.6 lm/w, calculated by the equation above. It means this phosphor is suitable for white LEDs as blue-emitting phosphor.

Conclusions

A series of $Ba_{4-x}OCl_6$: Eu^{2+}_x(x=0, 0.01, 0.03, 0.05, 0.07, 0.09) blue-emitting phosphors with good thermal stability and tiny chromaticity shift were systematically investigated. The integrated emission intensity at 423 K still remains 83.7% compared to the room temperature. The absolute quantum efficiency is up to 83.37%. The chromaticity shift remains the same with the test temperature rising from 350-490 K and is smaller than the commercial blue phosphor BAM. The luminous efficiency of the radiation (LER) of $Ba_{3.97}OCl_6$:$Eu^{2+}_{0.03}$ is 23.6 lm/w. At the same time, Eu^{2+} in the host of Ba_4OCl_6 has efficient broad absorption in ultraviolet region and give an intense blue emission. The result above indicates that this phosphor has potential application in the in (n)-UV LEDs.

Acknowledgements

This work was financially supported by grants from China Postdoctoral Science Foundation (No. 2014M562237), the Joint Funds of the National Natural Science Foundation of China (NNSFC) and Guangdong Province (No. U1301242), “973”programs (No.2014CB643801), Research Fund for the Doctoral Program of Higher Education of China (RFDP) (No. 20130171130001), the Government of Guangdong Province for Industrial Applications of Rare Earth Photoluminescence Materials (No. 2012B091000026 and 2013A090100010), teamwork Projects of Guangdong Natural Science Foundation (No. S2013030012842), Guangdong Provincial Science & Technology Project (No. 2013B090800019 and 2013Y2-00118), Natural Science Foundation of Guangdong Province (No. 2014A030313114), China Postdoctoral Science Foundation (No. 2014M562237), and the Fundamental Research Funds for the Central Universities (No. 14lgqt02).

Notes and references

1 M. Shang, C. Li and Jun Lin, *Chem. Soc. Rev.,* 2014, **43**, 1372; M. Peng, X. Yin, P. A. Tanner, C. Liang, P. Li, Q. Zhang, J. Qiu, *J. Am. Ceram. Soc.* 2013, **96**, 2870; C. Lu, H. Hong, R.

Jaganathan, *J Mater Chem.,* 2002, **12,** 2525; X. Mi, J. Sun, P. Zhou, H. Zhou, D. Song, K. Li, M. Shang and J. Lin, *J. Mater. Chem. C,* 2015, **3,** 4471.

2 Y. Chen, J. Wang, X. Zhang, G. Zhang, M. Gong and Q. Su, *Sensor. Actuat. B,* 2010, **148**, 259; D. Geng, M. Shang, Y. Zhang, H. Lian, J. Lin, *Inorg. Chem.* 2013, **52,** 13708; K. N. Shinde, S. J. Dhoble, A. Kumar, *Bull. Mater. Sci.*, 2011,**34,** 937; S. Unithrattil, K. Lee, W. H. Chung, W. B. Im, *J. Lumin.,* 2014, **152,** 176.

3 W. Huang, F. Yoshimura, K. Ueda, Y. Shimomura, H. Sheu, T. Chan, H. Greer, W. Zhou, S. Hu, R. Liu and J. Paul Attfield. *Angew. Chem.,* 2013, **125**, 8260; U. Kaufmann, M. Kunzer, K. Kohler, H. Obloh, W. Pletschen, P. Schlotter, R. Schmidt, J. Wagner, A. Ellens, W. Rossner, and M. Kobusch, *phys. stat.sol.,* 2001, **188**, 143; K. Sohn, D. Park, S. Cho, J. Kwak, and J. Kim, *Chem. Mater.,* 2006, **18***,* 1768; S. Ye, F. Xiao, Y. Pan, Y. Ma, Q. Zhang, *Mater. Sci. Eng.,* 2010, **71,** 1; M. Peng, X. Yin, P. Tanner, M. Brik and P. Li, *Chem. Mater.,* 2015, **27,** 2938.

4 Y. Wang and Z. Zhang. *Electrochem. Solid stat. Lett.,* 2005, **11**, H97; P. Zhu, Q. Zhu, H. Zhu, H. Zhao, B. Chen, Y. Zhang, X. Wang, W. Di, *Opt. Mater.*, 2008, **30,** 930.

5 K. Kim, Y. Kim, H. Chun, T. Cho, J. Jung, and J. Kang. *Chem. Mater.,* 2002, **14***,* 5045.

6 A. A. Coelho, *Topas Academic,* version 4, Brisbane, Australia, 2005.

7 O. Reckewea, F. DiSalvo, *J. chem. Sci.,* 2011, **66**, 1000.

8 R. Shannon, *Acta Crystallogr,* 1976, **A32,** 751; C. Lin, Z. Xiao, G. Guo, T. Chan and R. Liu, *J. Am Chem. Soc.,* 2010,**132,** 3020.

9 G. Blasse, *Philips Res. Rep.,* 1969, **24**, 131; Y. Chen, J. Wang, C. Liu, X. Kuang and Q. Su, *Appl. Phys. Let.,* 2011, **98,** 081917; G. Blass, *Philips Res. Rep.,* 1969, **24,** 131.

10 B. Antipeuko, I. Bataev, V. Ermolaev, E. Lyubimov, and T. Privalova, *Opt. Spectrosc.,* 1970, **29**, 177.

11 S. Gwak, P. Arunkumar, and W. Im, *J. Phys. Chem. C*, 2014, **118,** 2686; Y. Chen, Y. Li, J. Wang, M. Wu and C. Wang, *J. Phys. Chem. C*, 2014, **118,** 12494.

12 Y. Chen, J. Wang, Chunmeng Liu, Xiaojun Kuang, and Q. Su. *Appl. Phys. Let.,* 2011, **98,** 081917.

13 N. Yedukondalu, Vikas D. Ghule, and G. Vaitheeswaran, *J. Chem. Phys.,* 2013, **138,** 174701.

14 W. Xiao, X. Zhang, Z. Hao, G. Pan, Y. Luo, L. Zhang, J. Zhang, *Inorg. Chem.,* 2015, **54**, 3189.

15 K. Li, M. Shang, H. Lian, J. Lin, *Inorg. Chem.,* 2015, **54**, 7992.

16 Z. Wu, S. Wang, J. Liu, J. Yin, S. Kuang, *J. Alloy. Comp.,* 2015, **644**, 274.

17 S. Zhang, Y. Nakai, T. Tsuboi, Y. Huang, H. Jin Seo, *Inorg. Chem.,* 2015, **50**, 2897.

18 C. Huang, Y. Chiu, W. Liu, *Eur. J. Inorg. Chem.*, 2014. **23.** 3674-3680

19 D. Geng, M. Shang, Y. Zhang, H. Lian, Z. Cheng, J. Lin, *J. Mater. Chem. C*, 2013, **1,** 2345; R. Pang, C. Li, L. Shi and Q. Su, *J. Phys. Chem. Solids*, 2009, **70,** 303; S. Zhang, Y. Nakai, T. Tsuboi, Y. Huang and H. Seo, *Chem. Mater.,* 2011, **23,** 1216; B. Tian, B. Chen, Y. Tian, X. Li, J. Zhang, J. Sun, H. Zhong, L. Cheng, S. Fu, H. Zhong, Y. Wang, X. Zhang, H. Xia and R. Hua, *J. Mater. Chem. C*, 2013, **1,** 2338.

20 X. Zhang, L. Huang, F. Pan, M. Wu, J. Wang, Y. Chen, and Q. Su, *ACS Appl. Mater. Interfaces,* 2014, **6,** 2709; C. Tsai, W. Cheng, J. Chang, L. Chen, J. Chen, Y. Hsu, and W. Cheng*, J. Disp. Technol.,* 2013, **9,** 427–432. X. Zhang, J. Wang, L. Huang, F. Pan, Y. Chen, B. Lei, M. Peng and M. Wu, *ACS Appl. Mater. Interfaces,* 2015, **7,** 10044.

21 P. Smet, A. Parmentier, P. Dirk, *J Electrochem. Soc.,* 2011, **158,** R 37; Y. Chen, M. Wang, J. Wang, M. Wu, and C. Wang, *J. Solid State Lighting,* 2014, **1,** 5.

The table of contents (TOC) graphic

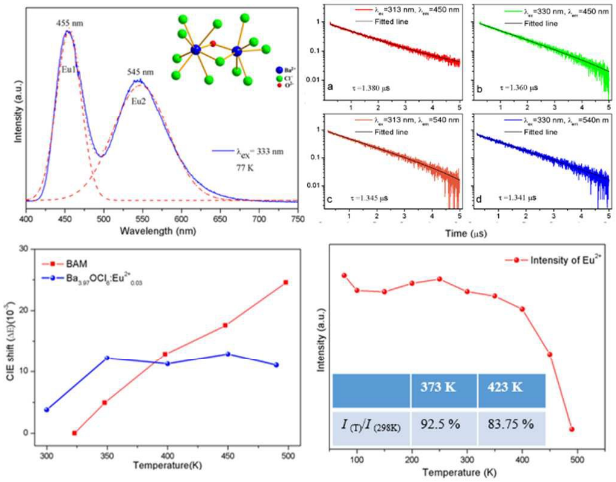

We develop an intense blue emitting phosphor Ba_4OCl_6: Eu^{2+} with tiny chromaticity shift. It shows good thermal stability and tiny chromaticity shift. The integrated emission intensity at 373 K and 423 K still remains 92.5 and 83.7%, compared with the intensity at room temperature.